Construction and Experimental Validation of a Petri Net Model of Wnt/β-Catenin Signaling

Annika Jacobsen[1,2,3]*, Nika Heijmans[4], Folkert Verkaar[3,5], Martine J. Smit[3,5], Jaap Heringa[1,2,3‡], Renée van Amerongen[4‡], K. Anton Feenstra[1,2,3‡]

1 Centre for Integrative Bioinformatics (IBIVU), VU University Amsterdam, Amsterdam, The Netherlands, **2** Department of Computer Science, VU University Amsterdam, Amsterdam, The Netherlands, **3** Amsterdam Institute for Molecules, Medicines and Systems, VU University Amsterdam, Amsterdam, The Netherlands, **4** Section of Molecular Cytology and Van Leeuwenhoek Centre for Advanced Microscopy, Swammerdam Institute for Life Sciences, University of Amsterdam, Amsterdam, The Netherlands, **5** Division of Medicinal Chemistry, VU University Amsterdam, Amsterdam, The Netherlands

‡ JH, RvA, and KAF are joint senior authors on this work.
* annika.jacobsen.86@gmail.com

Abstract

The Wnt/β-catenin signaling pathway is important for multiple developmental processes and tissue maintenance in adults. Consequently, deregulated signaling is involved in a range of human diseases including cancer and developmental defects. A better understanding of the intricate regulatory mechanism and effect of physiological (active) and pathophysiological (hyperactive) WNT signaling is important for predicting treatment response and developing novel therapies. The constitutively expressed CTNNB1 (commonly and hereafter referred to as β-catenin) is degraded by a destruction complex, composed of amongst others AXIN1 and GSK3. The destruction complex is inhibited during active WNT signaling, leading to β-catenin stabilization and induction of β-catenin/TCF target genes. In this study we investigated the mechanism and effect of β-catenin stabilization during active and hyperactive WNT signaling in a combined *in silico* and *in vitro* approach. We constructed a Petri net model of Wnt/β-catenin signaling including main players from the plasma membrane (WNT ligands and receptors), cytoplasmic effectors and the downstream negative feedback target gene *AXIN2*. We validated that our model can be used to simulate both active (WNT stimulation) and hyperactive (GSK3 inhibition) signaling by comparing our simulation and experimental data. We used this experimentally validated model to get further insights into the effect of the negative feedback regulator AXIN2 upon WNT stimulation and observed an attenuated β-catenin stabilization. We furthermore simulated the effect of APC inactivating mutations, yielding a stabilization of β-catenin levels comparable to the Wnt-pathway activities observed in colorectal and breast cancer. Our model can be used for further investigation and viable predictions of the role of Wnt/β-catenin signaling in oncogenesis and development.

Introduction

The Wnt/β-catenin signaling pathway is crucial for regulating cell proliferation and differentiation during embryonic development, while in adults it helps control tissue homeostasis and injury repair in stem cell maintenance [1, 2]. Extracellular WNT ligands activate signaling leading to CTNNB1 (commonly and hereafter referred to as β-catenin) stabilization, nuclear translocation, interaction with TCF/LEF transcription factors [3] and induction of β-catenin/TCF target genes [4] (Fig 1B). A critical feature of Wnt/β-catenin signaling is the inhibition of a 'destruction complex' which degrades the constitutively expressed β-catenin (Fig 1A) [5].

The destruction complex consists of two scaffolding proteins, AXIN1 and adenomatous polyposis coli (APC), and two kinases, casein kinase 1 (CK1) and glycogen synthase kinase 3 (GSK3). β-catenin is phosphorylated by CK1 and GSK3 [6, 7] and thereafter presented to the proteasome for ubiquitination [8] and degradation (Fig 1A). Extracellular WNT binds to and activates the 7 transmembrane receptor, Frizzled (FZD) [9], and the co-receptor, lipoprotein receptor-related protein (LRP5/6) [10]. The intracellular tail of FZD interacts with Dishevelled (DVL) through an incompletely understood mechanism and sequesters AXIN1 to the cell membrane [11] forming a so-called 'signalosome' [12]. This leads to depletion of the cytoplasmic pool of the destruction complex component AXIN1, which in turn inhibits the formation of the destruction complex itself (Fig 1B). It is not fully understood whether only AXIN1 or more destruction complex components are sequestered to the cell membrane during WNT signaling. Indeed, a study by Li *et al.* [13] showed that AXIN1 does not dissociate from the other destruction complex components during WNT signaling.

The inhibition of the destruction complex leads to β-catenin stabilization and nuclear translocation. Nuclear β-catenin interacts with TCF/LEF transcription factors [14] forming the β-catenin/TCF transcriptional (co)activator complex. A collection of more than 100 genes induced by β-catenin/TCF transcription is listed on the WNT homepage [15]. The specific subset of genes induced, however, strongly depends on tissue type and developmental stage [16]. Several of these target genes are feedback regulators, where *AXIN2* is of particular interest. First, *AXIN2* is a universal β-catenin/TCF target gene and as such it is believed to faithfully report Wnt-pathway activity in multiple tissues [17, 18]. Second, AXIN2 encodes a functional homolog of the destruction complex component AXIN1 [19] and mediates an auto-inhibitory feedback loop. Although AXIN1 and AXIN2 share functional similarities, they are only partially redundant *in vivo* due to their different expression patterns [20]: *AXIN1* is constitutively expressed [21], whereas *AXIN2* is induced during active Wnt/β-catenin signaling [18, 22]. The AXIN2 negative feedback is believed to be important for the tight spatio-temporal regulation of Wnt/β-catenin signaling [23]. However, the exact regulatory role of AXIN2 remains an open question.

Deregulated Wnt/β-catenin signaling caused by genetic alterations can have major developmental consequences, and is the leading cause of colorectal carcinogenesis [24]. The most common colorectal cancer mutation is found in APC [25, 26]. Different APC inactivating mutations lead to different levels of Wnt-pathway activity e.g. higher β-catenin stabilization is seen in colorectal cancer compared to breast cancer (as reviewed in [27]). Other rarer colorectal cancer mutations [28] are found in AXIN1 [29], AXIN2 [30, 31] and β-catenin [32, 33]. As a common mode of action, these oncogenic mutations cause hyperactive WNT signaling [34].

Investigating the mechanism and effect of β-catenin stabilization during physiological (active) and pathophysiological (hyperactive) WNT signaling is crucial for developing effective treatment, both in the field of cancer research and regenerative medicine. *In vitro* experiments in which cells are stimulated with WNT are generally assumed to represent active signaling, whereas downstream oncogenic mutations represent hyperactive signaling. Inhibition of GSK3 using small molecule inhibitors is widely used to activate WNT signaling during cellular
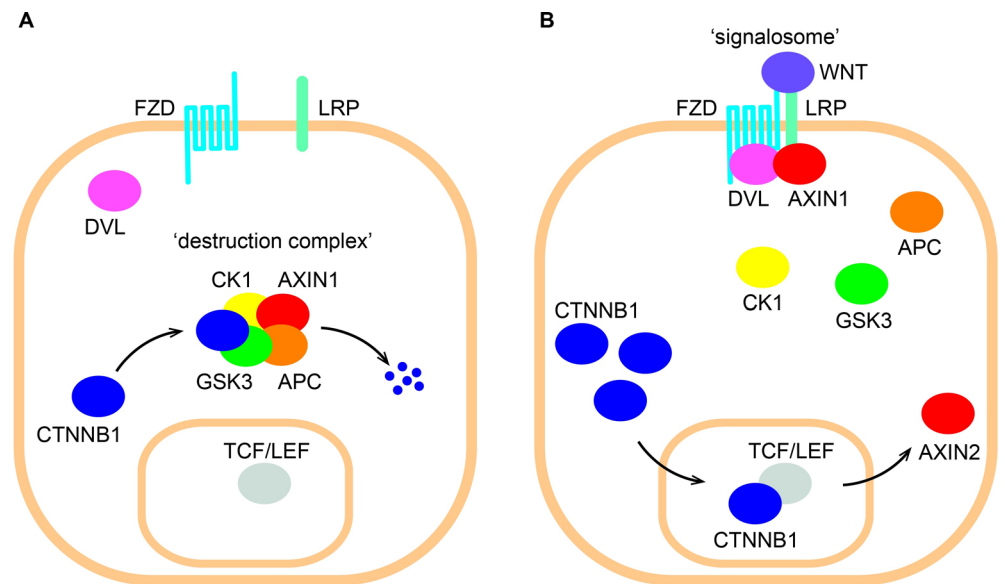
Fig 1. Illustration of Wnt/β-catenin signaling. (A) In the absence of an external WNT stimulus β-catenin (referred to by its official gene name CTNNB1 in the figure) is continuously degraded by a 'destruction complex' consisting of AXIN1, adenomatous polyposis coli (APC), casein kinase 1 (CK1) and glycogen synthase kinase 3 (GSK3). (B) Extracellular WNT interacts with the membrane-bound receptors frizzled (FZD) and lipoprotein receptor-related protein (LRP). Dishevelled (DVL) interacts with the intracellular tail of FZD and sequesters AXIN1 to the plasma membrane forming a so-called 'signalosome'. The ensuing depletion of the cytoplasmic pool of AXIN1 inhibits the formation of the destruction complex. β-catenin thereby stabilizes and translocates to the nucleus, where it interacts with TCF/LEF transcription factors activating transcription of specific target genes, including the negative feedback regulator *AXIN2*.

doi:10.1371/journal.pone.0155743.g001

reprogramming and in embryonic stem cell cultures [35, 36]. Inhibition of GSK3 inhibits the destruction complex, which can be interpreted as similar to the effects of oncogenic mutations. Several quantitative mathematical models of Wnt/β-catenin signaling have been created as reviewed in [37, 38] to facilitate these investigations. The first model [39] described the cytosolic interactions in WNT signaling based on data from experiments using *Xenopus* extracts. Later models included amongst other, extensions with (i) AXIN2 feedback, explaining effects of mutations in colorectal cancer [40]; (ii) AXIN2 feedback and another negative upstream feedback, demonstrating how these feedbacks ensure robust oscillations [41]; (iii) WNT inhibitors, secreted Frizzled-related protein and Dickkopf, which showed a synergistic effect on β-catenin accumulation [42]; (iv) effects of different target gene regulations induced by different WNT and APC concentrations [43]; (v) the interplay between adhesive and transcriptional functions of β-catenin [44] and (vi) data from experiments using mammalian cells, showing significant differences in AXIN levels [45]. However, constructing such quantitative models remains a challenge, because they require detailed information on e.g. protein concentrations and reaction rates. In addition to being dependent on large experimental efforts, these data are particularly difficult to obtain for a signaling pathway that does not involve a typical kinase cascade. Consequently, these models include many estimated parameters, which limits their scale of applicability [37]. Petri net models, on the other hand, use coarse-grained data describing currently known interactions and relative protein levels [46, 47]. A clear advantage of this is that such coarse-grained data are more readily available, and much easier to obtain. Coarse-grained Petri net models thus expand the scale of applicability for future modeling purposes, including extensions to novel signaling components or pathways.

Here we have used a combined computational and experimental approach to build the first Petri net model of Wnt/β-catenin signaling. Compared to the aforementioned mathematical

models, it includes a larger number of core Wnt-pathway components. Most importantly, we have included a signaling module that captures the interactions occurring at the cell membrane. As a result, our model allows both physiological (i.e. WNT ligand induced) and pathophysiological (i.e. induced by oncogenic mutations in downstream signaling components) to be captured. Furthermore, our model offers the possibility of including the negative feedback by AXIN2. We used the model to explain how active signaling upon WNT stimulation and hyperactive signaling upon GSK3 inhibition leads to different levels of β-catenin stabilization. We corroborated our observations from the model using data from TCF/LEF luciferase reporter assays and Western blot analysis. We then used the experimentally validated model to explore plausible modes of action of β-catenin stabilization as a result of negative feedback by activating expression of AXIN2 upon WNT stimulation, or due to APC inactivating mutations that are known to play a key role in oncogenesis of colorectal and breast cancer.

Results

Building a Petri Net Model for Wnt/β-Catenin Signaling

A Petri net model can be graphically represented with two types of nodes: 'places', describing the biological components, and 'transitions', describing the activity between the biological components, which can be constructed based on known interaction data. The places are denoted with 'tokens', which describe the relative availability of the biological component. Tokens are assigned on the basis of existing data from the literature, typically relative protein levels. Places and transition are connected by weighted arcs that are important for the flow of the network. [48–50] (see Materials and Methods for a detailed explanation of Petri nets).

We created a Petri net model of Wnt/β-catenin signaling to investigate the mechanism and effect of β-catenin stabilization under physiological (e.g. embryonic development) and pathophysiological (e.g. cancer) conditions based on the literature as described in details below (Fig 2). The model describes the interactions between the core proteins in the pathway with a focus on capturing the immediate behavior of β-catenin stabilization following destruction complex inactivation. Therefore the degradation of β-catenin by the destruction complex is specifically included in the model, while no changes in the production/degradation rate of the other proteins needed to be assumed. Likewise, the gene expressions of *β-catenin* (encoding β-catenin), but also of *AXIN2*, a negative feedback target gene of the Wnt-pathway, are also specifically included in the model. Production and degradation of all other proteins are assumed to have similar rates and are therefore omitted, such that the token levels of these proteins remain the same throughout the simulation (as detailed in Materials and Methods).

The final model consists of 18 places (circles, representing gene or protein states), 11 transitions (boxes, representing protein complex formation, dissociation, translocation or gene expression) and 41 arcs (arrows, representing the direction of flow of the tokens). In the model, WNT initiates signaling extracellularly by binding to its transmembrane receptors FZD and LRP (t1), forming the WNT/FZD/LRP complex. DVL interacts with the intracellular tail of FZD when present in the WNT/FZD/LRP complex (t2), forming the WNT/FZD/LRP/DVL complex. DVL thereafter sequesters AXIN1 to the membrane (t3) forming the signalosome consisting of WNT, FZD, LRP, DVL and AXIN1. In the model we have not specifically included the contribution of GSK3 and CK1 in the formation of the signalosome, because these two multi-tasking kinases are generally assumed not to be rate-limiting in the cell [24, 39]. Further, AXIN1 is the only destruction complex constituent that binds to the signalosome in the model. The signalosome dissociates once every 10 steps (t4) into the WNT/FZD/LRP/DVL complex and AXIN1 in order to incorporate a lower dissociation- than formation-rate of the signalosome. The destruction complex, which sequesters β-catenin unless WNT induces
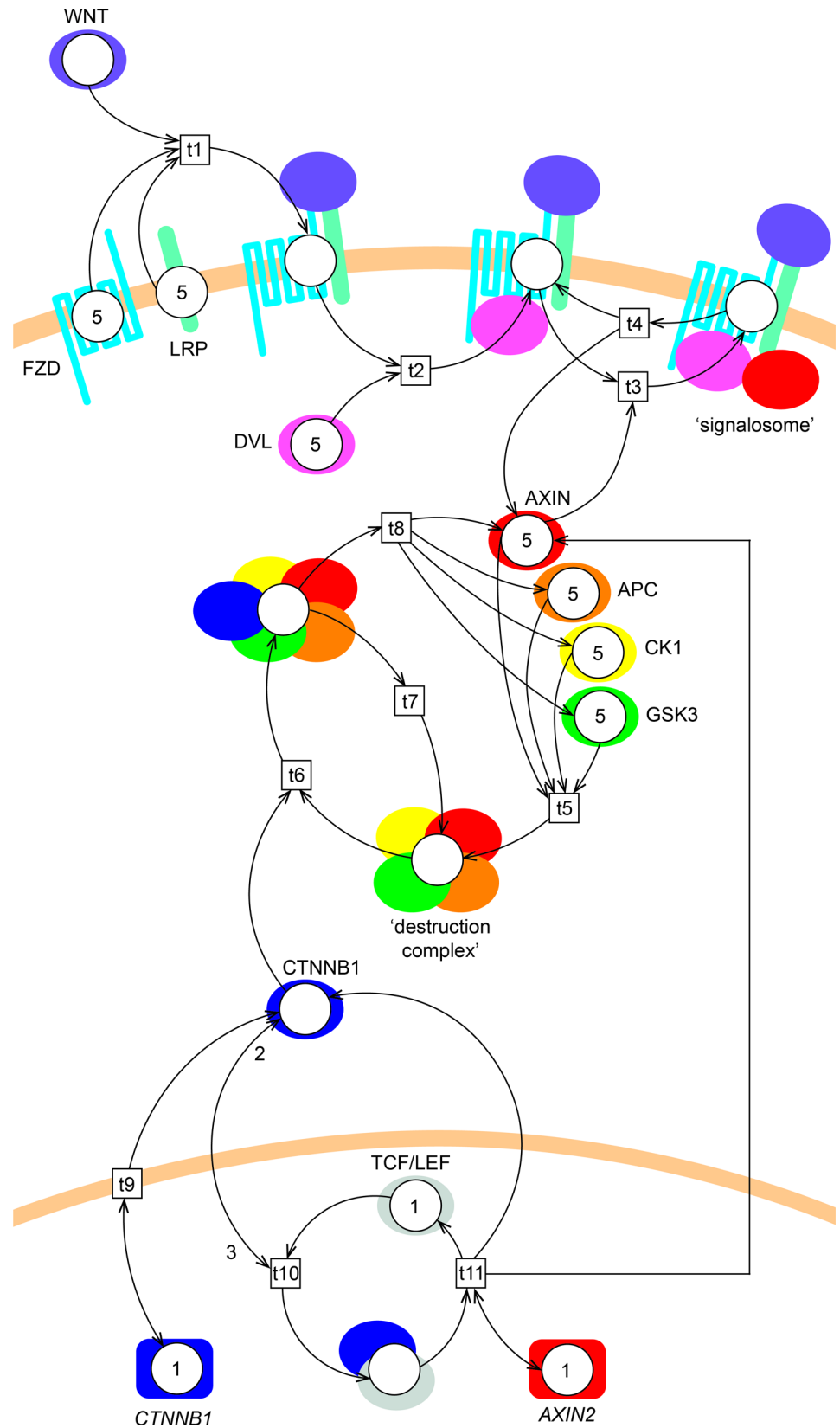
Fig 2. Petri net model of Wnt/β-catenin signaling. The model consists of 18 places (circles, representing gene or protein states), 11 transitions (boxes, representing protein complex formation, dissociation, translocation or gene expression) and 41 arcs (arrows, representing the direction of flow of the tokens). WNT initiates signaling by binding to FZD and LRP, forming the WNT/FZD/LRP complex. DVL and AXIN1 then interact with this complex intracellularly (t2 and t3, respectively) forming a so-called 'signalosome'. The signalosome dissociates (with a rate of once every 10 steps) into WNT/FZD/LRP/DVL and AXIN1 (t4). Note that β-catenin is referred to by its official gene name CTNNB1 in the figure. The β-catenin protein is produced every step (t9) by the *β-catenin* gene. AXIN1, APC, CK1 and GSK3 interact (t5) and form a 'destruction complex'. The destruction complex binds β-catenin (t6) to mark it for degradation. The destruction complex is then either reused (t7) for another round of β-catenin degradation or dissociates (t8) into its components AXIN1, APC, CK1 and GSK3. Alternatively, β-catenin may interact with TCF/LEF in the nucleus (t10), leading to transcriptional activation of *AXIN2* (t11). Initial token levels are 0 (not shown), 1 or 5 (depicted in the places). Most arc weights are 1 (not shown), except for the nuclear translocation and interaction of β-catenin to TCF/LEF transcription factors, which has an incoming arc weight of 3 and an outgoing arc weight of 2 (depicted on the arcs).

doi:10.1371/journal.pone.0155743.g002

signalosome formation, is formed (t5) by AXIN1, APC, CK1 and GSK3. In the model, β-catenin binding to the destruction complex leads to degradation of β-catenin (t8 and t7), and the destruction complex is then either reused (t7) for another round of β-catenin degradation or dissociates (t8) to AXIN1, APC, CK1 and GSK3. In the model, β-catenin protein is produced every step (t9) following transcription of the *β-catenin* gene, and either binds the destruction complex (t6) or translocates to the nucleus, where it interacts with TCF/LEF (t10) to activate transcription of *AXIN2* (t11). Since AXIN1 and AXIN2 are functional homologs [19], they are modeled as one protein entity (depicted as 'AXIN'). Further, we do not distinguish between the cytoplasmic and nuclear pool of β-catenin in the model. This allowed the nuclear translocation and TCF/LEF interactions to be modeled as one transition (t10).

The initial token level of the protein places were set to 5 (with exceptions described below) in order to have a concise but sufficiently large pool of the protein tokens for the model to work with. Higher levels had no effect, and lower levels restricted the expressiveness of the model, i.e. too coarse-grained. The initial token level of the β-catenin protein place and all protein complexes (WNT/FZD/LRP, WNT/FZD/LRP/DVL, signalosome, destruction complex-β-catenin and TCF/LEF-β-catenin) were set to 0, because these are produced throughout the simulation and are assumed to be initially absent. The initial token level of TCF/LEF was set to 1 which gives the lowest rate of TCF/LEF-β-catenin interaction, and hence the induction of low levels of AXIN2 [51]. A parameter sweep of initial token levels of TCF/LEF confirmed that higher initial token levels resulted in a stronger response and higher AXIN2 levels. Initial token levels of the gene places, *β-catenin* and *AXIN2*, were set to 1 and kept at these values since these genes are always presumed to be present. In our model this means that *AXIN2* is induced only when the TCF/LEF-β-catenin complex is present and *β-catenin* is induced once every step, because there is nothing implemented to restrain this induction (β-catenin levels are instead regulated by the destruction complex).

Most arc weights were set to 1, which means that the model dynamics rely on its connectivity. This has been proven successful using Petri net modeling of MAPK and AKT signaling cascades [46, 47, 52]. An exception to this was applied when implementing fractional arc weights to represent a lower transition rate (i.e. the dissociation of the signalosome, the effects of different APC mutations and the induction of AXIN2) and when implementing a higher interaction affinity of β-catenin to the destruction complex than to TCF/LEF. For the latter the arc weight from β-catenin to t10 (i.e. its translocation to the nucleus and subsequent interaction with TCF/LEF) was set to 3, and the arc weight from t10 to β-catenin was set to 2. From the model point of view this means that for t10 to fire, the β-catenin place needs to be occupied by 3 tokens, but only 1 is consumed (See Fig 2). These weights were chosen because it is generally assumed that β-catenin accumulates in the cytoplasm before it translocates to the nucleus and

binds TCF/LEF (as reviewed in [53]). This assumption is based on the higher interaction affinities of β-catenin to the destruction complex compared to TCF/LEF (as reviewed in [54]), which means that β-catenin will interact with TCF/LEF when the β-catenin levels begin to increase because the destruction complex is unable to keep up with the degradation. In order to implement the lower dissociation rate of the signalosome, the ingoing and outgoing arcs of t4 were implemented with a fractional arc weight of 0.1, which represents a firing rate of once every 10 steps. Further, we implemented a constraint on the transition to ensure that it does not fire more than once every step. Parts of this initial setup were changed accordingly to mimic the different conditions of Wnt/β-catenin signaling simulated in this study (see below).

Active Signaling upon WNT Stimulation

We simulated WNT stimulation to predict the level of β-catenin stabilization during active signaling. To this end we ran a series of simulations with different initial WNT token levels (ranging from 0 to 5) without AXIN2 feedback (i.e. the arc weight from t11 to AXIN was set to 0). As shown in Fig 3A, we observed four different β-catenin response levels depending on the initial WNT token level. A flat β-catenin response was seen for WNT = 0, 1 or 2. For WNT = 3, 4 or 5, we observed a delay in the initial increase of β-catenin, which eventually increased linearly with a slope depending on the WNT level. The β-catenin stabilization was low for WNT = 3 and moderate for WNT = 4 and 5. Maximal WNT stimulation (WNT = 5) led to a stabilization of ∼60 β-catenin tokens.

To compare the response predicted by our model to the biological response of cells treated with Wnt3a, we measured β-catenin activation by both Western blot analysis and TCF/LEF luciferase reporter assay (Fig 3B–3F and S1 Fig). Although the former directly detects β-catenin levels, the latter faithfully reports Wnt/β-catenin signaling [55] and remains the most sensitive and robust method to quantify Wnt/β-catenin signaling to date [15, 56, 57]. Furthermore, it allows high-throughput analyses of Wnt-pathway activation (i.e. a comparison of multiple doses and time points within the same experiment). To validate the β-catenin levels predicted upon WNT stimulation by our model, we treated HEK293T^WOO cells (carrying a stably integrated β-catenin/TCF luciferase reporter) with increasing concentrations of purified, commercially available, Wnt3a for 3, 8 and 24 hours. These experiments reproduce the dose- and time-dependent increase of TCF/LEF reporter gene activity predicted by our model (Fig 3B and 3C). To directly link the results from the reporter gene assay to an increase in β-catenin protein levels, we repeated the experiment for one level of WNT stimulation (100 ng/ml purified Wnt3a) for a more extensive time series, including additional earlier time points, and analyzed the results by performing both a TCF/LEF reporter gene assay (Fig 3B and 3D) and quantitative Western blot analysis (Fig 3E and 3F), which allows direct, albeit less sensitive, detection of β-catenin protein levels. Both the transcriptional reporter assay and the measurement of β-catenin protein levels show a time-dependent increase (Fig 3D–3F). Direct comparison of the two readouts reveals the inherent limitations of each of the two experimental systems: The change (i.e. fold increase) in TCF/LEF reporter activity is more pronounced than, but slightly delayed compared to, the change in β-catenin protein levels. Our Petri net model (Fig 3A) shows the same qualitative effect: a consistent rise in β-catenin levels. As such, our model more closely mimics the luciferase response (i.e. activation of an artificial reporter gene).

Hyperactive Signaling upon GSK3 Inhibition

To predict the level of β-catenin stabilization during hyperactive signaling by a downstream perturbation, we next simulated our model upon GSK3 inhibition. We ran a series of simulations with different initial GSK3 token levels (ranging from 5 to 0), where 5 initial tokens
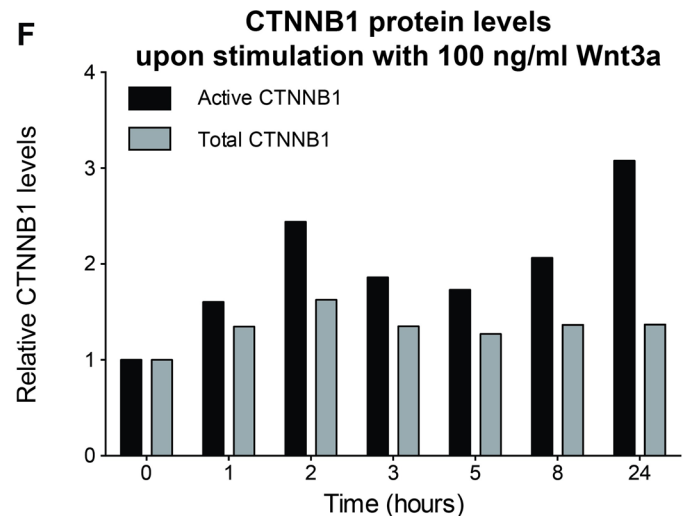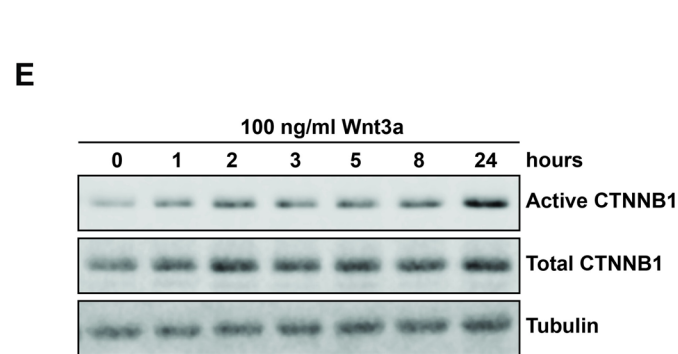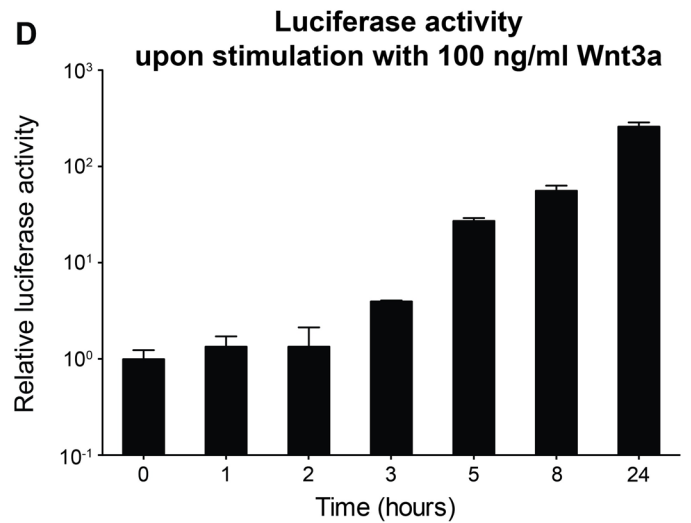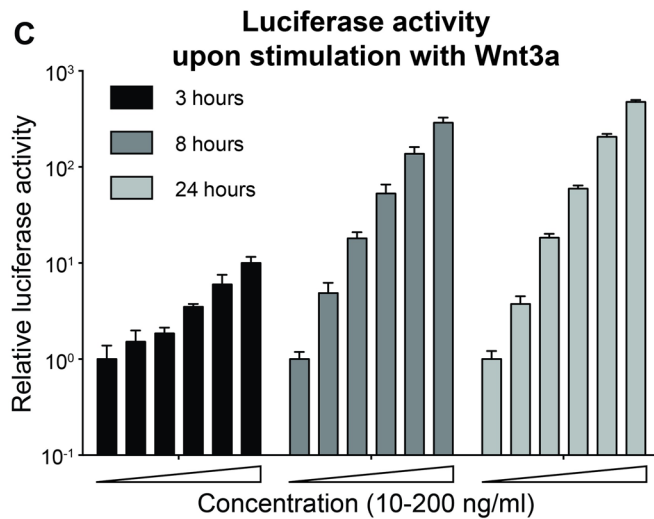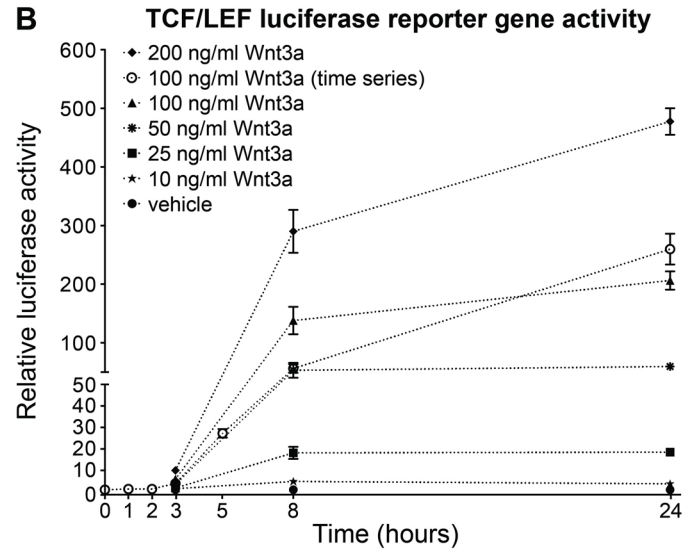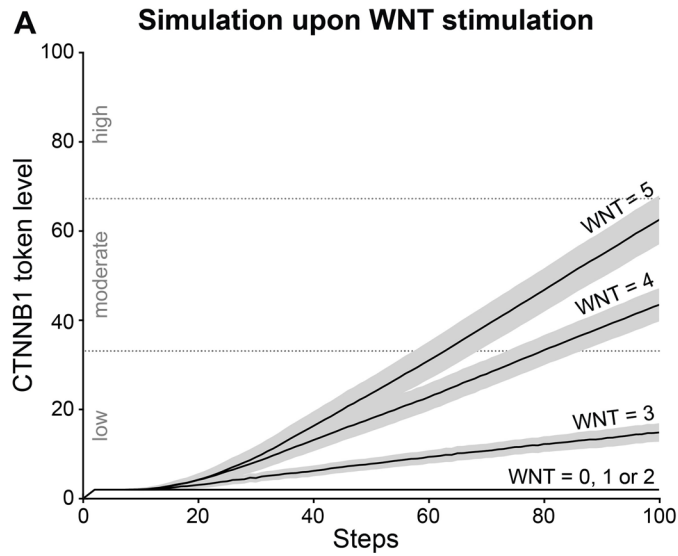
Fig 3. Model simulation and experimental validation of Wnt-pathway activation upon WNT stimulation. (A) β-catenin (referred to by its official gene name CTNNB1 in the figure) token levels predicted by our model with initial WNT token levels ranging from 0 to 5. For WNT = 0, 1 or 2, we observed a flat β-catenin response. For WNT = 3, 4 and 5 β-catenin increases from low to moderate levels. (B) Graph combining the results from panels C and D to allow easy comparison to the modeling results depicted in panel (A), showing dose- and time-dependent activation of a Wnt/β-catenin responsive TCF/LEF luciferase reporter in HEK293T^{WOO} cells. For all curves with black data points (corresponding to panel C), luciferase activity was plotted relative to the vehicle control (not shown), which was set at 1 for each of the three time points (3, 8 and 24 hours). For the curve with white data points (corresponding to panel D), luciferase activity was plotted relative to the vehicle control, which was set at 1 for the t = 0 hours condition. (C) Reporter assay in HEK293T^{WOO} cells, showing dose-dependent activation at 3, 8 and 24 hours after stimulation with purified Wnt3a (same concentrations as depicted in B). (D) Reporter assay in HEK293T^{WOO} cells, showing time-dependent activation upon treatment with 100 ng/ml of Wnt3a. Values were plotted relative to the vehicle control, which was set at 1 for t = 0 hours. (E) Western blot from the experiment depicted in (D), showing total and active (i.e. non-phosphorylated) β-catenin levels. Since the soluble, signaling pool of β-catenin constitutes only a minor fraction of the total pool of β-catenin, the use of antibody against active β-catenin ensures that only the pool involved in WNT signaling is visualized. Tubulin was used as a loading control. (F) Quantification of the Western blot shown in (E). Total and active β-catenin levels were normalized to tubulin. The increase in either total or active β-catenin levels was plotted relative to time point 0, for which the normalized levels were set to 1. Experiments were repeated two (C) or three (D-F) times. A representative experiment is shown.

represents wildtype (i.e. no Wnt-pathway activity) and 0 corresponds to complete inhibition (hyperactive signaling). The simulations revealed that the response levels depend on initial GSK3 token levels (see Fig 4A). For GSK3 = 3, 4 or 5, we observed a flat β-catenin response. A linear increase in β-catenin levels with a slope depending on GSK3 levels was seen for GSK3 = 0, 1 or 2. This corresponds to β-catenin degradation ranging from no degradation to 1 or 2 β-catenin tokens degraded per three simulation steps, respectively. Consequently, β-catenin stabilization was low for GSK3 = 2, moderate for GSK3 = 1 and high for GSK3 = 0. Complete GSK3 inhibition led to a stabilization of 100 β-catenin tokens.

To validate the coarse-grained β-catenin levels predicted by our model upon GSK3 inhibition, we stimulated HEK293T^{WOO} cells with increasing concentrations of CHIR99021, one of the most potent and selective GSK3 inhibitors available to date [58], over a broad time range (3, 8 and 24 hours). The measured TCF/LEF reporter gene activity confirmed the dose- and time-dependent increase upon GSK3 inhibition (Fig 4B and 4C) predicted by our model (Fig 4A). As with the Wnt3a treatment, here we also performed a TCF/LEF reporter gene assay and quantitative Western blot analysis side by side for one of the treatment conditions (3 μM CHIR99021) for multiple time points. The 3 μM CHIR99021 concentration was chosen in order to achieve a near maximal GSK3 inhibition or Wnt-pathway activation. An increase in both active (i.e. non-phosphorylated) and total (i.e. both phosphorylated and non-phosphorylated) β-catenin is apparent after 1 hour, whereas an increase in the signal of the luciferase reporter assay can only be detected after 3 hours. Furthermore, the dynamic range of the Western blot analysis is limited compared to the reporter gene assay, allowing us to measure at most a 4-fold increase in β-catenin levels in the former, but up to a 10^4 fold increase in Wnt-pathway activity in the latter (Fig 4D–4F).

Predictions of Hyperactive Signaling by APC Inactivating Mutations

The most common colorectal oncogene, *APC*, perturbs downstream WNT signaling. Different APC mutations exist that result in truncated proteins negatively influence the formation of the destruction complex to different degrees. As a result, the different APC mutations lead to different levels of β-catenin stabilizations. According to a recent review [27], the β-catenin signaling activity (β-catenin reporter activity) was low (between 10–20%) for APC mutations in breast tumors, versus moderate to high (between 20–100%) in colorectal tumors.

We used our validated model to explore if the effect of these APC mutations might be explained by different rates of destruction complex formation. We implemented the effect of the APC mutations by decreasing the rate of the destruction complex formation ranging from no production at all to production every 20, 10 and 5 steps. In Fig 5 we observed four different

A — Simulation upon GSK3 inhibition

B — TCF/LEF luciferase reporter gene activity

C — Luciferase activity upon stimulation with CHIR99021

D — Luciferase activity upon stimulation with 3 μM CHIR99021

E — 3 μM CHIR99021

F — CTNNB1 protein levels upon stimulation with 3 μM CHIR99021
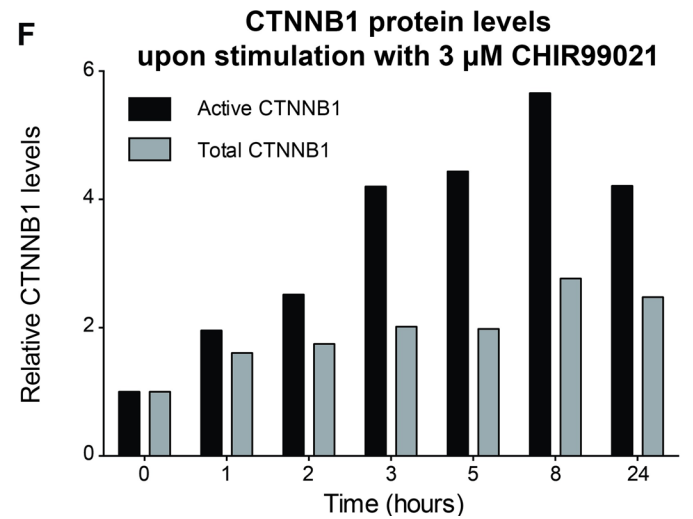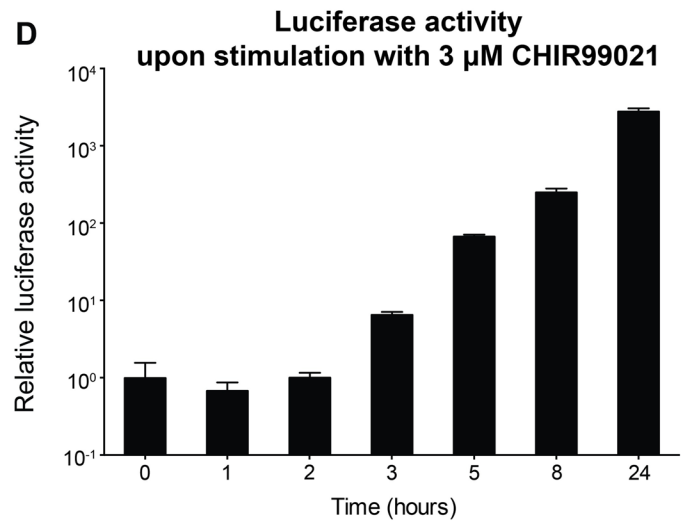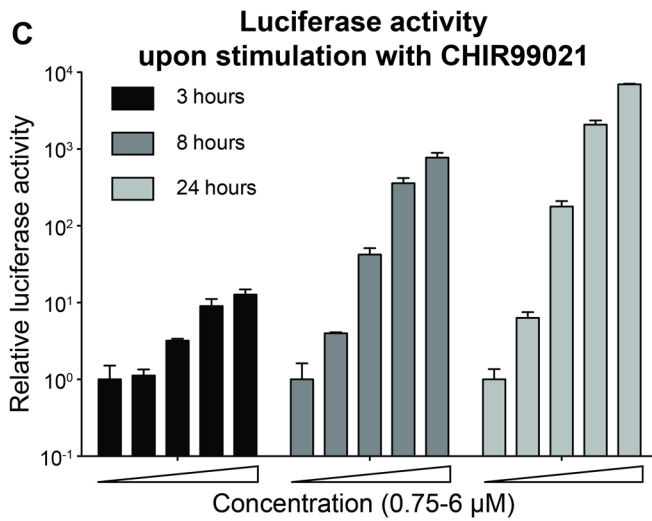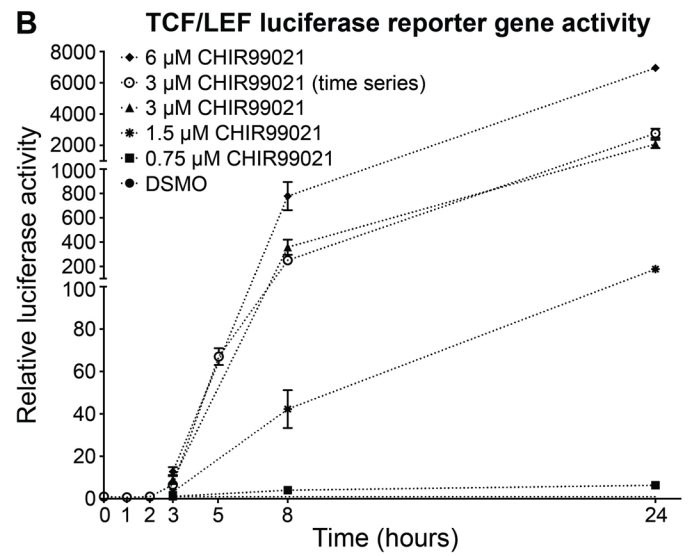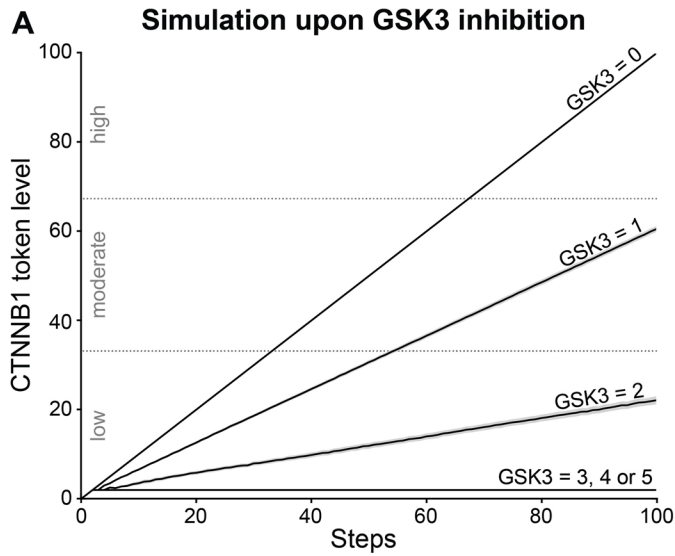
Fig 4. Model simulation and experimental validation of Wnt-pathway activation upon GSK3 inhibition. (A) β-catenin (referred to by its official gene name CTNNB1 in the figure) token levels predicted by our model with initial GSK3 token levels ranging from 0 to 5. For GSK3 = 3, 4 or 5, we observed a flat β-catenin response. For GSK3 = 0, 1 or 2 β-catenin increases to low, moderate or high levels, respectively. (B) Graph combining the results from panels C and D to allow easy comparison to the modeling results depicted in panel (A), showing dose- and time-dependent activation of a Wnt/β-catenin responsive TCF/LEF luciferase reporter in HEK293T^WOO cells. For all curves with black data points (corresponding to panel C), luciferase activity was plotted relative to the vehicle control (not shown), which was set at 1 for each of the three time points (3, 8 and 24 hours). For the curve with white data points (corresponding to panel D), luciferase activity was plotted relative to the vehicle control, which was set at 1 for the t = 0 hours condition. (C) Reporter assay in HEK293T^WOO cells, showing dose-dependent activation at 3, 8 and 24 hours after stimulation with CHIR99021 (same concentrations as depicted in B). (D) Reporter assay in HEK293T^WOO cells, showing time-dependent activation upon treatment with 3 μM CHIR99021. Values were plotted relative to the DMSO control, which was set at 1 for t = 0 hours. (E) Western blot from the experiment depicted in (D), showing total and active (non-phosphorylated) β-catenin levels. Tubulin was used as a loading control. (F) Quantification of the Western blot shown in (E). Total and active β-catenin levels were normalized to tubulin. The increase in either total or active β-catenin levels was plotted relative to time point 0, for which the normalized levels were set to 1. Experiments were repeated two (C) or three (D-F) times. A representative experiment is shown.

doi:10.1371/journal.pone.0155743.g004

response levels for the different APC mutations, where stabilization of β-catenin levels went from low to high depending on this rate of destruction complex formation. Comparing these token levels to the β-catenin signaling activities reviewed in [27], the three highest β-catenin stabilizations would correspond to hyperactive signaling by APC mutations in colorectal tumor formation (moderate and high β-catenin token levels), whereas the lowest β-catenin stabilization would correspond to the effects by APC mutations as observed in breast tumor formation (low β-catenin token levels).

Predictions of Active Signaling upon WNT Stimulation with AXIN2 Feedback

In our model *AXIN2* is induced by β-catenin/TCF transcription and increases the cytoplasmic pool of AXIN, which under certain conditions, e.g. WNT stimulation, is the limiting factor for β-catenin degradation. However, our experimental dataset obtained using Wnt3a stimulation showed no obvious decrease in β-catenin levels that might be due to this negative feedback (Fig 3E and 3F). It should be noted that in this experimental setting (100 ng/ml Wnt3a), the Wnt-pathway is likely still activated at supra-physiological levels. Moreover, the WNT ligand remains present throughout the experiment. *In vivo*, however, physiological Wnt-pathway activation is strictly regulated both due to the WNT concentration gradient and due to the tight
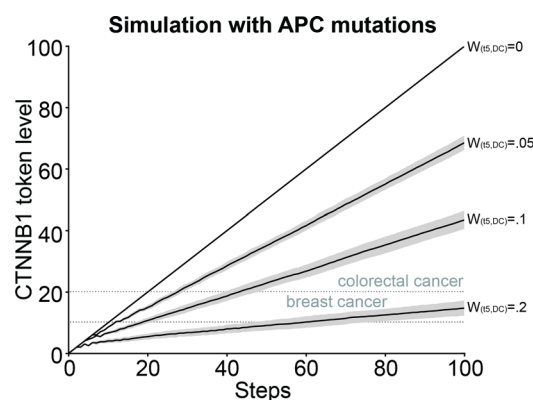
Fig 5. Model prediction of Wnt-pathway hyperactivation by APC inactivating mutations. β-catenin (referred to by its official gene name CTNNB1 in the figure) token levels predicted by our model with four different APC mutations (weight on the arc going from t5 to the destruction complex (DC) set at 0.2, 0.1, 0.05 and 0, respectively). Moderate and high β-catenin stabilizations might correspond to the effects by mutations in colorectal tumor formation and the low β-catenin stabilizations might correspond to the effects by mutations in breast tumor formation.

doi:10.1371/journal.pone.0155743.g005
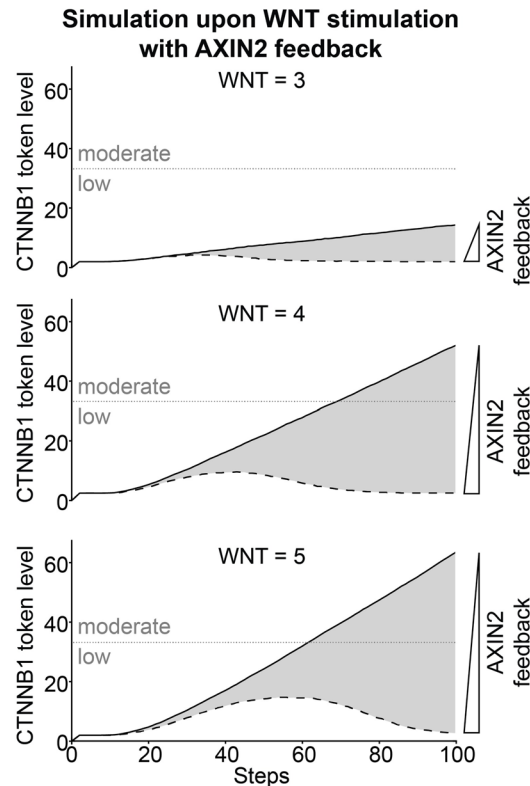
Fig 6. Model prediction of Wnt-pathway activation upon WNT addition with AXIN2 feedback. β-catenin (referred to by its official gene name CTNNB1 in the figure) token levels predicted by our model with arc weight from t11 to AXIN varied from 0 (no feedback; solid lines) to 0.15 (high feedback, dashed lines), and initial WNT token levels at 3, 4 and 5 (top, middle and bottom panels, respectively). We observed three spectra of β-catenin stabilizations depending on initial WNT levels. The highest β-catenin stabilizations correspond to simulations without AXIN2 feedback (solid lines), whereas with high AXIN2 feedback the β-catenin stabilization was attenuated (dashed lines).

doi:10.1371/journal.pone.0155743.g006

spatio-temporal control of Wnt gene expression. Under these circumstances, lower levels of Wnt/β-catenin signaling are likely to occur and, as a result, part of the regulation may be due to the AXIN2 auto-inhibitory feedback loop. Therefore, it may be the ratio between the WNT and AXIN2 levels that is crucial to the regulatory role of AXIN2. We therefore used our model to get further insights into the effect of the AXIN2 feedback and explored a spectrum of possible β-catenin stabilizations under different WNT and AXIN2 levels. We ran a series of simulations with different initial WNT token levels: 3, 4 or 5, which showed increased β-catenin stabilization in Fig 3A, and with different AXIN2 feedback strengths: the arc weight from t11 to AXIN was from 0 for no feedback to 0.15 for maximum feedback. As shown in Fig 6, we observed three different spectra of β-catenin stabilizations depending on the different initial WNT token levels. The highest β-catenin stabilizations (solid lines in Fig 6) were identical to those observed in Fig 3A (without AXIN2 feedback). At high feedback, the β-catenin stabilization is lowered, and a maximum appears after which the β-catenin level declines (dashed lines in Fig 6). The lowest β-catenin stabilizations displayed three different peak responses. For the peak responses, the height of the peak and the duration of the response depended on initial WNT token levels. Maximal β-catenin stabilization comes later in the simulation for higher initial WNT token levels.

Discussion

In spite of more than 30 years of study, the Wnt/β-catenin signaling pathway still holds many questions. The molecular details of how an external WNT stimulus results in the stabilization of transcriptionally active β-catenin/TCF complexes remain incompletely understood and, in some cases, a topic of debate [59]. The Petri net model presented in this paper allows us to investigate downstream effects of Wnt/β-catenin signaling under physiological and pathophysiological conditions. The core of the model describes the current state of knowledge as summarized in the introduction. The coarse-grained nature of the interaction and protein level data used to build our model allowed us to include the interactions at the plasma membrane, which is lacking from currently existing quantitative models as reviewed in [37, 38]. Of note, AXIN1 is the only destruction complex component sequestered to the plasma membrane during Wnt/β-catenin signaling in our model. For now we ignored the actions of GSK3 at the plasma membrane, where it phosphorylates LRP5/6 to create the AXIN1 binding site and where, in turn, the kinase itself may be inhibited [60, 61]. Furthermore, we considered free cytoplasmic and nuclear β-catenin as a single pool in the model. More detailed experimental data on subcellular compartmentalization of β-catenin (or any other signaling component) would allow us to refine our Petri net model, which easily allows incorporation of such detail. For instance, at present our model only considers the active (i.e. unphosphorylated), rather than the total pool of β-catenin, which would also include the β-catenin present in the adhesion complexes in the cell membrane.

Our Petri net model for Wnt/β-catenin signaling was constructed based on known interactions of signaling components described in the literature, thereby capturing the current state of knowledge in the field. To validate the model, we generated our own experimental data. This allowed a direct comparison of physiological (i.e. WNT stimulation) and pathophysiological (i.e. GSK3 inhibition) activation of the pathway in the same cell line, using time points and analyses best suited for connecting our experimental data and the Petri net modeling predictions.

Our model predicts a dose- and time dependent response for both WNT stimulation and GSK3 inhibition (Figs 3A and 4A). This is confirmed by the experimental data (Figs 3B, 3C, 4B and 4C). The main discrepancy between the simulated and the experimental data is the time-delay that is predicted in response to WNT stimulation compared to GSK3 inhibition (compare Figs 3A–4A). Indeed, activation of Wnt/β-catenin signaling is known to be a slow event (unlike the activation of MAPK signaling for instance, which occurs within a matter of minutes) [62–64]. However, we did not detect this delay in β-catenin accumulation by either TCF/LEF luciferase reporter assay (compare Fig 3B–3D to Fig 4B–4D) or Western blot analysis (compare Fig 3E and 3F to Fig 4E and 4F). We believe this is mainly due to experimental limitations. Given that a subtle increase in β-catenin protein levels can be detected approximately one hour after stimulation with either Wnt3a (Fig 3E and 3F) or CHIR99021 (Fig 4E and 4F), any delay in activation of the Wnt-pathway must occur prior to that time point. Detecting this delay would require assays with superior spatio-temporal resolution. The delay predicted by our model upon WNT stimulation (Fig 3A) can be explained by the fact that formation of the signalosome occurs a few steps into the simulation, whereas inhibition of GSK3 is a one-step event, and that the transitions for signalosome formation (i.e. pathway activation) and destruction complex formation (i.e. pathway inhibition) compete for AXIN1. Thus, when AXIN1 is sequestered to the plasma membrane, less cytoplasmic AXIN1 is available for formation of the destruction complex. To what extent these events contribute to Wnt-pathway activation under experimental conditions remains unknown, owing to the absence of tools to study the exchange of endogenous AXIN1 between these two pools. Our results do suggest that

competition over AXIN1 between the destruction complex and the signalosome may well be important also under physiological conditions.

The time-delay together with the continuous sequestration and dissociation of AXIN1 to the signalosome leads to prediction of higher stabilization of β-catenin for complete GSK3 inhibition compared to maximal WNT stimulation, where the difference is almost two-fold (compare Figs 4A–3A). We observe a similar difference when measuring TCF/LEF reporter gene activity: the highest concentration of CHIR99021 activates the reporter approximately 10-fold higher than the highest concentration of Wnt3a tested (compare Fig 4B–4D to Fig 3B–3D). Comparing protein levels, instead of transcriptional activation, shows a much smaller difference: 2-fold higher β-catenin at most when cells are stimulated with CHIR99021 versus Wnt3a (compare Fig 4E and 4F to Fig 3E and 3F). Although it is tempting to conclude that this data again confirms the predictions of our model, it should be stressed that the different experimental modes of Wnt-pathway activation cannot be compared directly. This is because they are achieved by different molecules (i.e. purified Wnt3a versus a synthetic small-molecule GSK3 inhibitor) with different intrinsic activities and chemical properties such as half-life and stability in the tissue culture medium, which may greatly impact on the experimental outcome. At the same time, we may speculate that the observed differences reflect real differences in sensitivity of the Wnt-pathway. In this case, our experimental findings might be explained by the fact that the more physiological means of pathway activation by Wnt3a is more likely to be subject to negative feedback control via AXIN2 induction than the more artificial perturbation by CHIR99021 inhibition of GSK3 at the level of the destruction complex.

AXIN2 is one of the few comprehensive globally expressed WNT target genes and is thought to act as a negative regulator to Wnt/β-catenin signaling [17, 18]. The degree to which AXIN2 attenuates WNT signaling and the actual spatio-temporal regulatory role of AXIN2 is still a topic of debate. Indeed, when we incorporate this negative feedback loop in the model upon WNT stimulation, our simulations predict that Wnt-pathway activity is attenuated (at certain levels of AXIN2 induction), and ultimately returns to baseline levels (dashed lines in Fig 6). Importantly, in the model the feedback from AXIN2 only negatively influences stabilized β-catenin levels when AXIN1 is the limiting factor. This is the case when AXIN1 is deprived from the cytoplasm by sequestration to the signalosome (i.e. upon WNT stimulation). This is why we are able to observe a negative effect from the AXIN2 feedback upon WNT stimulation in our model (Fig 6), but not by GSK3 inhibition (Fig 4A) or APC inactivating mutations (Fig 5). It should be noted however, that on the timescale used for the experiments, we do not observe complete feedback inhibition by AXIN2 (Fig 3B–3F). This might be due to the relatively low level of *AXIN2* induction in the cells used for these experiments [51] in combination with supra-physiological levels of Wnt-pathway activation achieved upon stimulation with purified Wnt3a. However, it could also be due to the fact that AXIN1 is not the limiting factor in the cells used for this study. Previously, a study of Wnt/β-catenin signaling in *Xenopus laevis* showed that AXIN1 is 1000-fold lower than the other components of the destruction complex [39] and has therefore been considered the natural limiting factor. However, a recent study of Wnt/β-catenin signaling in mammalian cells showed that the concentrations of the components of the destruction complex were on the same range [45]. Therefore, we cannot exclude the possibility that AXIN1 is not the limiting factor in the cells used for this study. Unfortunately, the current experimental tools, most notably Western blot analysis of endogenous β-catenin levels, are not robust, high-throughput and sensitive enough to resolve this issue. However, by using our model we were able to predict and visualize spectra of β-catenin stabilization, which showed that the ratio between the WNT and AXIN2 levels are important for the degree of feedback observed (Fig 6). The two most notable observations were that, for high WNT levels, a higher level of AXIN2 was needed to reach baseline β-catenin levels and, for low WNT

levels, a baseline β-catenin level is reached early. Based on these predictions we can speculate whether the AXIN2 negative feedback only has an effect on low WNT levels and whether the regulatory role of this is to insure a faster on/off switch of Wnt-pathway activity. At present, in both our simulations and current experimental setting the cells are continuously exposed to Wnt3a. During normal development cells may essentially only receive a short pulse of WNT stimulation, given that the hydrophobic WNT proteins either do not travel far from their production source or are quickly sequestered by responsive cells. Indeed, in vivo Wnt-pathway activity shows dynamic on and off switches during development [23, 65, 66]. Examples of these are the restriction of Wnt/β-catenin responsive cells to the crypt, but not to the villus sections of the intestinal epithelium, and oscillation of WNT signaling as part of the mouse segmentation clock. By including protein degradation and different sources of WNT protein in our model, such oscillations might also be simulated.

In conclusion, our Petri net model of Wnt/β-catenin signaling provides insight on the mechanisms leading to different levels of β-catenin stabilization upon WNT stimulation and GSK3 inhibition corroborated by TCF/LEF luciferase assay and Western blot analysis. It should be stressed that the simulations show a coarse-grained output per step and we cannot directly map token levels to the relative activities in the TCF/LEF luciferase reporter assay nor to the β-catenin levels measured by Western blot analysis. Furthermore, we also cannot directly map a simulation step in the model to an experimental timescale. Despite these limitations, our model resembles Wnt/β-catenin signaling to the extent that it captures the logic of the interactions and reflects the sequence of events of pathway activation and repression by various mechanisms. In this way, our model can be used to simulate and predict both physiological and pathophysiological WNT signaling. Thus, this modeling exercise has allowed us to study the mechanisms and effects of Wnt/β-catenin signaling under different conditions, as well as the effects of protein- and pathway-modifications that are known to influence this pathway in many types of cancer.

Materials and Methods

Petri Net Modeling

We built a Petri net model of Wnt/β-catenin signaling describing known components, actions and interactions, well established in literature, in a logical way. A Petri net consists of two types of nodes, 'places' and 'transitions', and is connected by directed edges called 'arcs'. A place represents an entity (e.g. gene or protein), whereas a transition indicates the activity occurring between the places (e.g. gene expression or complex formation). Places can only link to transitions and vice versa (i.e., a Petri net is a bipartite graph). The direction of the arcs is important for the flow of the network. An arc goes from an input place to a transition, and from a transition to an output place. Places contain 'tokens', indicating the availability of the corresponding entity, while arcs have a weight, denoting the amount of tokens to consume from an input place or to produce to an output place. If the token levels of all input places of a transition fulfill the requirement of (i.e. are equal to or higher than) the weights of the respective arcs, the transition is enabled. Only enabled transitions can be executed, leading to transfer (consumption/production) of tokens between places. Note that if two (or more) enabled transitions share an input place, they may be in competition if available token levels do not allow simultaneous execution of both (or all). In our model, AXIN, β-catenin and the destruction complex with β-catenin bound, are each input places for two transitions (t3/t5, t6/t10 and t7/t8, respectively). The initial token levels and the arc weights are generally restricted to be integer values. However, to represent a lower firing rate of a transition (i.e. a rate-limiting step) a fractional arc weight is implemented.

Gene expression is modeled such that one arc goes from the gene-place to the transcriptional-transition, one arc goes from the transcriptional-transition to the gene-place, and one arc goes from the transcriptional-transition to the protein-place. Gene-places are initiated with 1 token and when the transcriptional-transition of a gene is enabled the token is produced both in the protein-place and in the gene-place itself. This way the token can be reused for another round of gene expression, reflecting the fact that the gene (DNA) is needed, but is not consumed during expression.

Active and Hyperactive Conditions in the Model

We modeled active and hyperactive signaling upon WNT stimulation and GSK3 inhibition, respectively, and used these conditions to validate the model with experimental data (see below). Inhibition of GSK3 inhibits formation of the destruction complex, which we interpret to be similar to oncogenic perturbations. Therefore, for modeling purposes, GSK3 inhibition was used to mimic hyperactive signaling. For GSK3 inhibition we varied the initial token level of GSK3, respectively, from 0 to 5. For WNT stimulation we varied the initial token level of WNT from 0 to 5 and removed the AXIN2 feedback (the arc weight from t11 to AXIN was set to 0). The experimentally validated model was used to predict the level of β-catenin stabilization with the AXIN2 negative feedback upon WNT stimulation and APC inactivating mutations, respectively. Upon WNT stimulation with the AXIN2 feedback we varied the initial token level of WNT (3, 4 and 5) and the arc weight from t11 to AXIN (0 (no feedback) and 0.15 (maximal feedback)). The maximal feedback of 0.15 was chosen based on the criteria that it should i) show a peak response and ii) return to basal level for all initial WNT token levels (3, 4 and 5). This arc weight represents a firing rate of three times every 20 steps. Thus, the simulation for each initial WNT token level produced two β-catenin stabilization curves (i.e. no feedback and maximal feedback). The area between these two curves was used to explain the spectra of β-catenin stabilizations at intermediate levels of *AXIN2* induction. APC mutants have decreased binding affinity to the other components of the destruction complex to different degrees. We implemented this by reducing the formation of the destruction complex i.e. the weight on the arc going from the complex-formation-transition (t5) to the destruction complex (production) was decreased to 0, 0.05, 0.1 and 0.2. In addition, we incorporated arcs going from the complex-formation-transition to the individual destruction complex components (i.e. AXIN1, APC, GSK3 and CK1) with arc weights of 1 minus the production-weight to equally decrease the consumption. The implemented arc weight of 0 represents no production of the destruction complex (i.e. a complete null mutation). The implemented fractional arc weights of 0.05, 0.1 and 0.2 represent a production of the destruction complex once every 20, 10 and 5 steps, respectively.

Simulations

The model was simulated with maximally parallel execution, cf. our previous work [47], where the maximum possible number of enabled transitions are executed at each simulation step. This mimics the behavior in the cell, where typically many interactions happen at the same time. Two or more transitions can compete over one input place, as mentioned above. If this place only contains enough tokens to enable one of the transitions, but not both, a conflict occurs which is resolved by randomly drawing one of the competing transitions to execute. This makes the simulations non-deterministic.

For each condition we simulated the total β-catenin token levels, i.e. free β-catenin and β-catenin bound to the destruction complex or TCF/LEF, respectively, over 100 steps repeated 100 times. To account for variations in token levels due to the non-deterministic nature of the

model, the mean and standard deviation of the β-catenin token levels over the 100 simulations were calculated for each step. These 100 steps represent the (early) time scale of β-catenin accumulation and the final token count represents the stabilized β-catenin level measured in experiments. The simulation steps describe the sequence of events and should not be linearly translated to time units. Similarly, the token level is a coarse-grained quantitative representation of actual protein levels and should not be linearly translated to a concentration. Instead, for analysis of the simulations we observe relative differences of β-catenin token levels over steps between simulations (i.e. different conditions and dosages). To validate the model we compared the relative β-catenin token levels predicted by our model simulations to the relative Wnt-pathway activities measured in the experiment (see below), where we distinguish between 'low', 'moderate' and 'high' levels. A Python script was written to run the simulations and is available together with the model in pnml format via http://www.ibi.vu.nl/downloads/WNTmodel/.

Cell Lines

HEK293T^{WOO} (WNT OFF/ON) cells were generated by transfecting HEK293T cells with a 7xTcf-FFluc//SV40-Puro^{R} (7TFP) reporter plasmid (a gift from Christophe Fuerer, [67]). Following puromycin selection to obtain stable integrants, individual clones were assessed for their response to Wnt-pathway activation. The clone with the highest dynamic range was used for the experiments depicted in Figs 3 and 4.

Cell Culture and Stimulation

HEK293T^{WOO} cells were cultured in Dulbecco's Modified Eagle Medium: Nutrient Mixture F-12 (DMEM/F12) supplemented with 10% FCS and 1% Penicillin/Streptomycin (GIBCO, Life Technologies) in 5% CO_2 at 37°C. These cells respond to activation of the Wnt/β-catenin signaling pathway by expressing firefly luciferase, since the firefly luciferase in the 7TFP construct is driven by the 7xTcf promoter, which contains 7 repeats of the TCF/LEF transcription response element. Cells were plated the day prior to stimulation in a 96 well-plate at a density of 20.000 cells per well. Cells were stimulated with different concentrations (10–200 ng/ml) of purified Wnt3a protein (RnD) dissolved in 0.1% BSA in PBS, or with different concentrations (750 nM-6 µM) CHIR99021 (BioVision) dissolved in DMSO, for different amounts of time (1–24 hours). At the indicated time points following stimulation, cells were lysed in 20 µl of Passive Lysis Buffer (Promega) and cell lysate from the same experiment was used for both the luciferase assay (3 wells per condition) and Western blot analysis (the remainder of the 3 wells, pooled per lane).

Western Blot Analysis

Protein concentration was measured using the Pierce BCA Protein Assay Kit (Thermo Fisher Scientific). Equal amounts of protein were run on an 8% SDS-PAGE gel. Proteins were transferred to a nitrocellulose membrane (Bio-Rad) and blocked with TBS Odyssey Blocking Buffer (LI-COR Biosciences, diluted 1:1 in TBS prior to use). Primary antibodies directed against active β-catenin (Cat# 8814S, Cell Signaling, 1:1000), total β-catenin (Cat# 610153, BD Biosciences, 1:2000) and α-Tubulin (Cat# T9026, Sigma-Aldrich, 1:500) were diluted in blocking buffer supplemented with 0.1% Tween-20 (TBS-T). Staining was performed overnight at 4°C. Membranes were washed in TBS-T followed by incubation with secondary antibodies (IRDye 680LT (Cat# 926–68021) or IRDye 800CW (Cat# 926–32212) (LI-COR), 1:20000 in TBS-T) for 2 hours. Membranes were washed in TBS-T and incubated in TBS prior to scanning at 700 nm and 800 nm using an Odyssey Fc (LI-COR Biosciences). Image Studio^{TM} Lite 4.0 software

(LI-COR Biosciences) was used to quantify relative protein levels. Background correction was performed according to the manufacturer's instructions (median of pixels, top/bottom border width of 3).

Luciferase Assay

To measure the activity of firefly luciferase (and hence Wnt-pathway activity), 10 µl of cell lysate was transferred to a black 96-well Optiplate (Perkin Elmer). The SpectraMax L Microplate Luminometer was used to inject 50 µl Luciferase Assay Reagent II (Promega) per well followed by measurement of firefly luciferase activity.

Supporting Information

S1 Fig. Illustration of the "location" of the experimental readouts of Western blot analysis and luciferase reporter assay. The "location" of the readouts of Western blot analysis and luciferase reporter assay compared to their equivalent implementation in our Petri net model. Western blot analysis measures the protein levels of β-catenin (i.e. measures the β-catenin accumulation), whereas the luciferase reporter assay measures the transcriptional activation (by β-catenin/TCF complexes) of the TOPFLASH reporter, which is followed by the production of luciferase protein. Since the luciferase reporter activation requires β-catenin to be present it takes longer for the TOPFLASH reporter to be activated than for the increase in β-catenin protein levels to occur i.e. the activation always occurs downstream of β-catenin accumulation.
(PDF)

Acknowledgments

Author Contributions

Conceived and designed the experiments: AJ NH FV MJS JH RvA KAF. Performed the experiments: AJ NH. Analyzed the data: AJ NH FV MJS JH RvA KAF. Contributed reagents/materials/analysis tools: AJ NH JH RvA KAF. Wrote the paper: AJ NH JH RvA KAF.

References

1. Clevers H, Nusse R. Wnt/β-catenin Signaling and Disease. Cell. 2012; 149: 1192–205. doi: 10.1016/j.cell.2012.05.012 PMID: 22682243

2. Cadigan KM, Peifer M. Wnt Signaling from Development to Disease: Insights from Model Systems. Cold Spring Harbor perspectives in biology. 2009; 1: a002881. doi: 10.1101/cshperspect.a002881 PMID: 20066091

3. Henderson BR, Fagotto F. The ins and outs of APC and β-catenin nuclear transport. EMBO Rep. 2002; 3: 834–9. PMID: 12223464

4. Mosimann C, Hausmann G, Basler K. β-catenin hits chromatin: regulation of Wnt target gene activation. Nature reviews Molecular cell biology. 2009; 10: 276–86. doi: 10.1038/nrm2654 PMID: 19305417

5. Stamos JL, Weis WI. The β-catenin Destruction Complex. Cold Spring Harbor perspectives in biology. 2013; 5: a007898. doi: 10.1101/cshperspect.a007898 PMID: 23169527

6. Amit S, Hatzubai A, Birman Y, Andersen JS, Ben-Shushan E, Mann M, et al. Axin-mediated CKI phosphorylation of β-catenin at Ser 45: a molecular switch for the Wnt pathway. Genes & development. 2002; 16: 1066–76.

7. Ikeda S, Kishida S, Yamamoto H, Murai H, Koyama S, Kikuchi A. Axin, a negative regulator of the Wnt signaling pathway, forms a complex with GSK-3β and β-catenin and promotes GSK-3β-dependent phosphorylation of β-catenin. EMBO J. 1998; 17: 1371–84. PMID: 9482734

8. Aberle H, Bauer A, Stappert J, Kispert A, Kemler R. β-catenin is a target for the ubiquitin–proteasome pathway. EMBO J. 1997; 16: 3797–804. PMID: 9233789

9. Bhanot P, Brink M, Samos CH, Hsieh J-C, Wang Y, Macke JM, et al. A new member of the frizzled family from Drosophila functions as a Wingless receptor. Nature. 1996; 382: 225–30. PMID: 8717036

10. Tamai K, Semenov M, Kato Y, Spokony R, Liu C, Katsuyama Y, et al. LDL-receptor-related proteins in Wnt signal transduction. Nature. 2000; 407: 530–5. PMID: 11029007

11. Schwarz-Romond T, Metcalfe C, Bienz M. Dynamic recruitment of axin by Dishevelled protein assemblies. Journal of cell science. 2007; 120: 2402–12. PMID: 17606995

12. Bilic J, Huang Y-L, Davidson G, Zimmermann T, Cruciat C-M, Bienz M, et al. Wnt Induces LRP6 SIgnalosomes and Promotes Dishevelled-Dependent LRP6 Phosphorylation. Science. 2007; 316: 1619–22. PMID: 17569865

13. Li VS, Ng SS, Boersema PJ, Low TY, Karthaus WR, Gerlach JP, et al. Wnt Signaling through Inhibition of β-catenin Degradation in an Intact Axin1 Complex. Cell. 2012; 149: 1245–56. doi: 10.1016/j.cell.2012.05.002 PMID: 22682247

14. Behrens J, von Kries JP, Kühl M, Bruhn L, Wedlich D, Grosschedl R, et al. Functional interaction of β-catenin with the transcription factor LEF-1. Nature. 1996; 382: 638–42. PMID: 8757136

15. Nusse R. Howard Hughes Medical Institute and the Department of Developmental Biology at Stanford University, California, USA; 2016. Available: http://web.stanford.edu/group/nusselab/cgi-bin/wnt/.

16. Buchert M, Athineos D, Abud HE, Burke ZD, Faux MC, Samuel MS, et al. Genetic Dissection of Differential Signaling Threshold Requirements for the Wnt/β-catenin Pathway In Vivo. PLoS genetics. 2010; 6: e1000816. doi: 10.1371/journal.pgen.1000816 PMID: 20084116

17. Lustig B, Jerchow B, Sachs M, Weiler S, Pietsch T, Karsten U, et al. Negative Feedback Loop of Wnt Signaling through Upregulation of Conductin/Axin2 in Colorectal and Liver Tumors. Molecular and cellular biology. 2002; 22: 1184–93. PMID: 11809809

18. Jho Eh, Zhang T, Domon C, Joo CK, Freund JN, Costantini F. Wnt/β-Catenin/Tcf Signaling Induces the Transcription of Axin2, a Negative Regulator of the Signaling Pathway. Molecular and cellular biology. 2002; 22: 1172–83. PMID: 11809808

19. Behrens J, Jerchow B-A, Würtele M, Grimm J, Asbrand C, Wirtz R, et al. Functional Interaction of an Axin Homolog, Conductin, with β-Catenin, APC, and GSK3β. Science. 1998; 280: 596–99. PMID: 9554852

20. Chia IV, Costantini F. Mouse Axin and Axin2/Conductin Proteins Are Functionally Equivalent In Vivo. Molecular and cellular biology. 2005; 25: 4371–6. PMID: 15899843

21. Zeng L, Fagotto F, Zhang T, Hsu W, Vasicek TJ, Perry WL, et al. The Mouse Fused Locus Encodes Axin, an Inhibitor of the Wnt Signaling Pathway That Regulates Embryonic Axis Formation. Cell. 1997; 90: 181–92. PMID: 9230313

22. Leung JY, Kolligs FT, Wu R, Zhai Y, Kuick R, Hanash S, et al. Activation of AXIN2 expression by β-catenin-T cell factor. A feedback repressor pathway regulating Wnt signaling. The Journal of biological chemistry. 2002; 277: 21657–65. PMID: 11940574

23. Aulehla A, Herrmann BG. Segmentation in vertebrates: clock and gradient finally joined. Genes & development. 2004; 18: 2060–7.

24. MacDonald BT, Tamai K, He X. Wnt/β-catenin signaling: components, mechanisms, and diseases. Developmental cell. 2009; 17: 9–26. doi: 10.1016/j.devcel.2009.06.016 PMID: 19619488

25. Polakis P. Wnt Signaling in Cancer. Cold Spring Harbor perspectives in biology. 2012; 4: a008052. doi: 10.1101/cshperspect.a008052 PMID: 22438566

26. Anastas JN, Moon RT. WNT signalling pathways as therapeutic targets in cancer. Nature reviews Cancer. 2013; 13: 11–26. doi: 10.1038/nrc3419 PMID: 23258168

27. Albuquerque C, Bakker ER, van Veelen W, Smits R. Colorectal cancers choosing sides. Biochimica et biophysica acta. 2011; 1816: 219–31. doi: 10.1016/j.bbcan.2011.07.005 PMID: 21855610

28. Fearon ER. Molecular Genetics of Colorectal Cancer. Annual review of pathology. 2011; 6: 479–507. doi: 10.1146/annurev-pathol-011110-130235 PMID: 21090969

29. Satoh S, Daigo Y, Furukawa Y, Kato T, Miwa N, Nishiwaki T, et al. AXIN1 mutations in hepatocellular carcinomas, and growth suppression in cancer cells by virus-mediated transfer of AXIN1. Nat Genet. 2000; 24: 245–50. PMID: 10700176

30. Liu W, Dong X, Mai M, Seelan RS, Taniguchi K, Krishnadath KK, et al. Mutations in AXIN2 cause colorectal cancer with defective mismatch repair by activating β-catenin/TCF signalling. Nat Genet. 2000; 26: 146–7. PMID: 11017067

31. Mazzoni SM, Fearon ER. AXIN1 and AXIN2 variants in gastrointestinal cancers. Cancer letters. 2014; 355: 1–8. doi: 10.1016/j.canlet.2014.09.018 PMID: 25236910

32. Morin PJ, Sparks AB, Korinek V, Barker N, Clevers H, Vogelstein B, et al. Activation of β-Catenin–Tcf Signaling in Colon Cancer by Mutations in β-Catenin or APC. Science. 1997; 275: 1787–90. PMID: 9065402

33. Rubinfeld B, Robbins P, El-Gamil M, Albert I, Porfiri E, Polakis P. Stabilization of β-Catenin by Genetic Defects in Melanoma Cell Lines. Science. 1997; 275: 1790–2. PMID: 9065403

34. Klaus A, Birchmeier W. Wnt signalling and its impact on development and cancer. Nature reviews Cancer. 2008; 8: 387–98. doi: 10.1038/nrc2389 PMID: 18432252

35. Ying QL, Wray J, Nichols J, Batlle-Morera L, Doble B, Woodgett J, et al. The ground state of embryonic stem cell self-renewal. Nature. 2008; 453: 519–23. doi: 10.1038/nature06968 PMID: 18497825

36. Li Y, Zhang Q, Yin X, Yang W, Du Y, Hou P, et al. Generation of iPSCs from mouse fibroblasts with a single gene, Oct4, and small molecules. Cell research. 2011; 21: 196–204. doi: 10.1038/cr.2010.142 PMID: 20956998

37. Lloyd-Lewis B, Fletcher AG, Dale TC, Byrne HM. Toward a quantitative understanding of the Wnt/β-catenin pathway through simulation and experiment. Wiley interdisciplinary reviews Systems biology and medicine. 2013; 5: 391–407. doi: 10.1002/wsbm.1221 PMID: 23554326

38. Kofahl B, Wolf J. Mathematical modelling of Wnt/β-catenin signalling. Biochem Soc Trans. 2010; 38(5): 1281–5. doi: 10.1042/BST0381281 PMID: 20863299

39. Lee E, Salic A, Krüger R, Heinrich R, Kirschner MW. The Roles of APC and Axin Derived from Experimental and Theoretical Analysis of the Wnt Pathway. PLoS biology. 2003; 1: E10. PMID: 14551908

40. Cho K-H, Baek S, Sung M-H. Wnt pathway mutations selected by optimal β-catenin signaling for tumorigenesis. FEBS letters. 2006; 580(15): 3665–70. PMID: 16764864

41. Wawra C, Kuhl M, Kestler HA. Extended analyses of the Wnt/β-catenin pathway: robustness and oscillatory behaviour. FEBS letters. 2007; 581(21): 4043–8. PMID: 17678900

42. Kogan Y, Halevi-Tobias Karin E, Hochman G, Baczmanska Anna K, Leyns L, Agur Z. A new validated mathematical model of the Wnt signalling pathway predicts effective combinational therapy by sFRP and Dkk. Biochemical Journal. 2012; 444(1): 115–25. doi: 10.1042/BJ20111887 PMID: 22356261

43. Benary U, Kofahl B, Hecht A, Wolf J. Modeling Wnt/beta-Catenin Target Gene Expression in APC and Wnt Gradients Under Wild Type and Mutant Conditions. Frontiers in physiology. 2013; 4: 21. doi: 10.3389/fphys.2013.00021 PMID: 23508686

44. van Leeuwen IM, Byrne HM, Jensen OE, King JR. Elucidating the interactions between the adhesive and transcriptional functions of β-catenin in normal and cancerous cells. Journal of theoretical biology. 2007; 247(1): 77–102. PMID: 17382967

45. Tan CW, Gardiner BS, Hirokawa Y, Layton MJ, Smith DW, Burgess AW. Wnt Signalling Pathway Parameters for Mammalian Cells. PloS one. 2012; 7: e31882. doi: 10.1371/journal.pone.0031882 PMID: 22363759

46. Bonzanni N, Garg A, Feenstra KA, Schutte J, Kinston S, Miranda-Saavedra D, et al. Hard-wired heterogeneity in blood stem cells revealed using a dynamic regulatory network model. Bioinformatics. 2013; 29: i80–8. doi: 10.1093/bioinformatics/btt243 PMID: 23813012

47. Bonzanni N, Krepska E, Feenstra KA, Fokkink W, Kielmann T, Bal H, et al. Executing multicellular differentiation: quantitative predictive modelling of C.elegans vulval development. Bioinformatics. 2009; 25: 2049–56. doi: 10.1093/bioinformatics/btp355 PMID: 19515963

48. Krepska E, Bonzanni, N, Feenstra, A, Fokkink, W, Kielmann, T, Bal, H, Heringa, J. Design Issues for Qualitative Modelling of Biological Cells with Petri Nets. Proceedings of the Formal Methods in Systems Biology 2008, Vol 5054 of LNBI, Springer, Cambridge, UK. 2008: 48–62.

49. Petri CA. Kommunikation mit Automaten. PhD Thesis, Technische Universität Darmstadt, Bonn, Germany. 1962.

50. Reisig CAR, G. Lectures on Petri Nets I: Basic Models, Vol. 1491 and 1492 of LNCS. Springer, Berlin, Germany. 1998.

51. de la Roche M, Worm J, Bienz M. The function of BCL9 in Wnt/beta-catenin signaling and colorectal cancer cells. BMC Cancer. 2008; 8: 199. doi: 10.1186/1471-2407-8-199 PMID: 18627596

52. Ruths D, Muller M, Tseng J-T, Nakhleh L, Ram PT. The Signaling Petri Net-Based Simulator: A Non-Parametric Strategy for Characterizing the Dynamics of Cell-Specific SIgnaling Networks. PloS CB. 2008; 4: e1000005.

53. Jamieson C, Sharma M, Henderson BR. Targeting the β-catenin nuclear transport pathway in cancer. Seminars in Cancer Biology. 2014; 27: 20–9. doi: 10.1016/j.semcancer.2014.04.012 PMID: 24820952

54. Harris TJC, Peifer M. Decisions, decisions: β-catenin chooses between adhesion and transcription. Trends Cell Biol. 2005; 15: 234–7. PMID: 15866026

55. Molenaar M, van de Wetering M, Oosterwegel M, Peterson-Maduro J, Godsave S, Vladimir K, et al. XTcf-3 Transcription Factor Mediates β-Catenin-Induced Axis Formation in Xenopus Embryos. Cell. 1996; 86: 391–9. PMID: 8756721

56. Veeman MT, Slusarski DC, Kaykas A, Louie SH, Moon RT. Zebrafish Prickle, a Modulator of Nonca-nonical Wnt/Fz Signaling, Regulates Gastrulation Movements. Current Biology. 2003; 13: 680–5. PMID: 12699626

57. van de Wetering M, Cavallo R, Dooijes D, van Beest M, van Es J, Loureiro J, et al. Armadillo Coacti-vates Transcription Driven by Product of the Drosophila Segment Polarity Gene dTCF. Cell. 1997; 88: 789–99. PMID: 9118222

58. Ring DB, Johnson KW, Henriksen EJ, Nuss JM, Goff D, Kinnick TR, et al. Selective GLycogen Synthase Kinase 3 Inhibitors Potentiate Insulin Activation of Glucose Transport and Utilization In Vitro and In Vivo. Diabetes. 2003; 52: 588–95. PMID: 12606497

59. Verkaar F, Cadigan KM, van Amerongen R. Celebrating 30 Years of Wnt Signaling. Science signaling. 2012; 5: mr2. doi: 10.1126/scisignal.2003714 PMID: 23233527

60. Davidson G, Wu W, Shen J, Bilic J, Fenger U, Stannek P, et al. Casein kinase 1γ couples Wnt receptor activation to cytoplasmic signal transduction. Nature. 2005; 438: 867–72. PMID: 16341016

61. Zeng X, Tamai K, Doble B, Li S, Huang H, Habas R, et al. A dual-kinase mechanism for Wnt co-receptor phosphorylation and activation. Nature. 2005; 438: 873–7. PMID: 16341017

62. Naik S, Piwnica-Worms D. Real-time imaging of β-catenin dynamics in cells and living mice. PNAS. 2007; 104:17465–70. PMID: 17954915

63. Yokoyama N, Yin D, Malbon CC. Abundance, complexation, and trafficking of Wnt/β-catenin signaling elements in response to Wnt3a. Journal of molecular signaling. 2007; 2:11. PMID: 17961224

64. Verkaar F, Blankesteijn WM, Smits JF, Zaman GJ. β-Galactosidase enzyme fragment complementa-tion for the measurement of Wnt/β-catenin signaling. FASEB journal: official publication of the Federa-tion of American Societies for Experimental Biology. 2010; 24: 1205–17.

65. Gonzalez A, Manosalva I, Liu T, Kageyama R. Control of *Hes7* expression by Tbx6, the Wnt pathway and the chemical Gsk3 inhibitor LiCl in the mouse segmentation clock. PloS one. 2013; 8(1): e53323. doi: 10.1371/journal.pone.0053323 PMID: 23326414

66. Suriben R, Fisher DA, Cheyette BN. Dact1 presomitic mesoderm expression oscillates in phase with Axin2 in the somitogenesis clock of mice. Dev Dyn. 2006; 235(11): 3177–83. PMID: 17013874

67. Fuerer C, Roel N. Lentiviral Vectors to Probe and Manipulate the Wnt Signaling Pathway. PloS one. 2010; 5: e9370. doi: 10.1371/journal.pone.0009370 PMID: 20186325